

# Synthesis and Characterization of a Two-Coordinate Manganese Complex and its Reaction with Molecular Hydrogen at Room Temperature\*\*

Prinson P. Samuel, Kartik Chandra Mondal, Herbert W. Roesky,\* Markus Hermann, Gernot Frenking,\* Serhiy Demeshko, Franc Meyer, A. Claudia Stückl, Jonathan H. Christian, Naresh S. Dalal, Liviu Ungur, Liviu F. Chibotaru, Kevin Pröpper†, Alke Meents, and Birger Dittrich\*

Dedicated to Professor Wolfgang A. Herrmann on the occasion of his 65th birthday

In 2005 we reported the first  $\text{LMn}-\text{MnL}$  compound ( $\text{L} = \text{CH}(\text{CMeNAr})_2$ ,  $\text{Ar} = 2,6\text{-}i\text{Pr}_2\text{C}_6\text{H}_3$ ) obtained by the reduction of  $\text{LMnCl}$  with sodium–potassium alloy. The resulting compound contains two three-coordinate Mn atoms.<sup>[1]</sup> We were curious about the electronic, magnetic, and chemical properties of the compound when the coordination number at the manganese atom is further reduced. Our recent success in stabilizing a silicon atom in a two-coordinate environment using cyclic alkyl(amino)carbene (cAAC) encouraged us to follow a similar synthetic strategy in order to prepare a compound with a two-coordinate manganese atom.<sup>[2]</sup> Such two-coordinate transition metals are very rare and only little studied in coordination chemistry. The main reason for the instability of these species with two-coordinate transition metals is the intermolecular association to satisfy the coordination requirements.<sup>[3]</sup> In recent years, chemists have made strong efforts to overcome this difficulty by using bulky ligands. The search for such coordinatively unsaturated transition-metal complexes has been driven mainly by their interesting magnetic features.<sup>[4]</sup> In addition to the unique magnetic behavior, enormous possibilities for elusive chemical reactions at a coordinatively unsaturated site make two-coordinate metal centers interesting for chemists. So far, only a few compounds with a two-coordinate manganese center

are known in the gaseous and solid phase, and complexes with linear geometry are rather uncommon.<sup>[5]</sup> The only reported complexes with two-coordinate manganese atoms and linear geometry in the solid phase are  $\text{Mn}[\text{C}(\text{SiMe}_3)_3]_2$  and  $\text{Mn}[\text{SAr}]_2$ , ( $\text{Ar} = \text{C}_6\text{H}_3\text{-}2,6\text{(C}_6\text{H}_2\text{-}2,4,6\text{-}i\text{Pr}_3)_2$ ). The latter compound exhibits secondary metal–ligand interactions.<sup>[5a–c]</sup> All the reported complexes with two-coordinate manganese ions are in their high-spin configuration with an  $S = \frac{5}{2}$  spin state and exhibit magnetic moments in the range of 5.1–6.0  $\mu_{\text{B}}$ . Herein we report a compound of composition (cAAC)<sub>2</sub>Mn (**2**) with a two-coordinate manganese atom and linear geometry, and with a magnetic moment of 4.15  $\mu_{\text{B}}$ , which reflects a total spin ground state of  $S_{\text{T}} = \frac{3}{2}$ . In addition, we also report the facile splitting of molecular hydrogen at the radical centers of **2**, resulting in the formation of (cAAC)<sub>2</sub>Mn (**3**) which shows an  $S = \frac{5}{2}$  spin state because of the quenching of the radical nature of the carbene ligand.

(cAAC)<sub>2</sub>MnCl<sub>2</sub> (**1**) was obtained by reacting cAAC: and MnCl<sub>2</sub> in a 1:1 ratio in THF at room temperature. The reaction of **1** with KC<sub>8</sub> and cAAC: in a 1:2.1:1 ratio afforded **2** as a deep-purple-colored product (Scheme 1). The X-ray structure of **2** shows a linear geometry with C–Mn–C = 180° (Figure 1). The Mn–C bond distance is 1.9655(14) Å, which is distinctly shorter than the corresponding bond length in

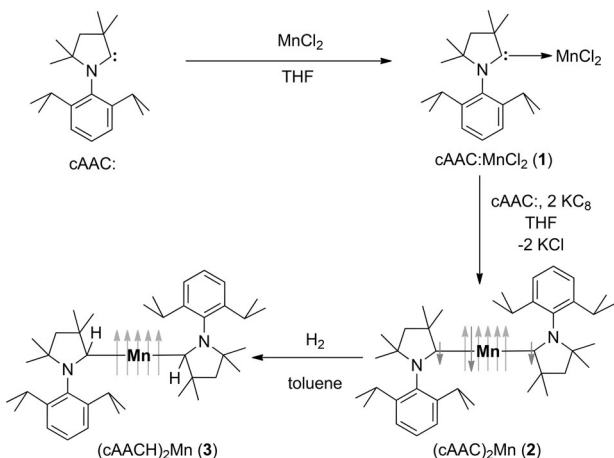
[\*] Dr. P. P. Samuel, Dr. K. C. Mondal, Prof. Dr. H. W. Roesky, Dr. S. Demeshko, Prof. Dr. F. Meyer, Dr. A. C. Stückl, Dr. K. Pröpper Institut für Anorganische Chemie, Georg-August-Universität Tammannstrasse 4, 37077 Göttingen (Germany)  
E-mail: hroesky@gwdg.de  
M. Hermann, Prof. Dr. G. Frenking Fachbereich Chemie, Philipps-Universität Marburg Hans-Meerwein-Str., 35032-Marburg (Germany)  
E-mail: frenking@chemie.uni-marburg.de  
J. H. Christian, Prof. Dr. N. S. Dalal Department of Chemistry and Biochemistry, Florida State University Tallahassee, FL 32306-4390 (USA)  
Dr. L. Ungur, Prof. L. F. Chibotaru KU Leuven Celestijnenlaan, 200F, 3001 Leuven (Belgium)  
Dr. A. Meents Deutsches Elektronen-Synchrotron Notkestraße 85, 22607 Hamburg (Germany)

Priv.-Doz. Dr. B. Dittrich  
Universität Hamburg  
Martin-Luther-King-Platz 6, 20146 Hamburg (Germany)  
E-mail: birger.dittrich@chemie.uni-hamburg.de

[†] K.P. passed away during the revision of this manuscript.

[\*\*] H.W.R. thanks the Deutsche Forschungsgemeinschaft for financial support (RO 224/60-1). We thank Kristian Dalle (F. Meyer research group) for UV/Vis measurements and Dr. A. P. Singh for preparing starting materials. L.U. is a postdoc of the Flemish Science Foundation (FWO). A part of this work was carried out at the PetralI light source at DESY, a member of the Helmholtz Association (HGF). We would like to thank Dr. Saravanan Panneerselvam for assistance in using beamline P11.

 Supporting information for this article is available on the WWW under <http://dx.doi.org/10.1002/anie.201304642>.



**Scheme 1.** Syntheses of compounds **1** and **2** and the facile splitting of dihydrogen by **2** to form **3**. Compound **2** shows a  $d^6$  electronic configuration at the Mn atom with one radical electron delocalized on two “carbene” carbon atoms.

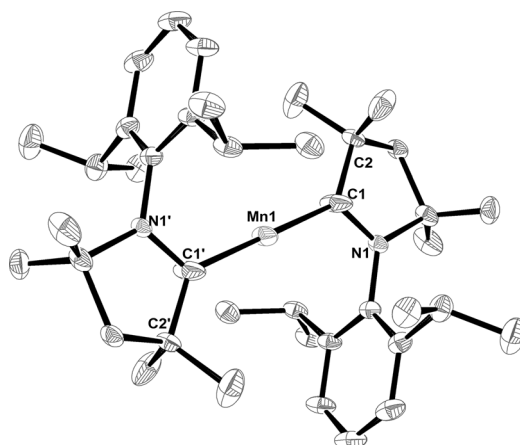


**Figure 1.** Molecular structure of compound **2**. Hydrogen atoms and solvent molecule (toluene) are omitted for clarity. Anisotropic displacement parameters are depicted at the 50% probability level. Selected experimental [calculated at BP86/def2-TZVPP for quartet<sup>[6]</sup>/sextet state] bond lengths [ $\text{\AA}$ ] and angles [ $^\circ$ ]: Mn1–C1 1.9655(14) [1.975; 1.978/1.984], C1–C2 1.5075(17) [1.540; 1.543/1.540], C1–N1 1.3589(16) [1.381; 1.383/1.377], C1–Mn1–C1' 180 [171.6/180.0], C2–C1–N1 107.82(10) [106.4; 106.9/106.6], C2–C1–Mn1 132.43(10) [124.5; 126.3/126.0], N1–C1–Mn1 119.75(10) [126.8; 128.9/127.4] N1–C1–C1'–N1' 180.0 [127.8/180.0].

$\text{Mn}[\text{C}(\text{SiMe}_3)_3]_2$  ( $2.102 \text{ \AA}$ ).<sup>[5a]</sup> The molecule possesses an inversion center at the manganese atom. Compound **2** is stable for several days at room temperature under an inert atmosphere, but decomposes readily on exposure to air. The stability of compound **2** with its less bulky cAAC: ligands tends to deviate from the hitherto existing assumption that very high steric hindrance is an essential requirement for the stabilization of compounds with two-coordinate manganese and linear geometry.

The magnetic moment of **2** is  $4.15 \mu_B$  at room temperature, that is, close to the spin-only value for  $S = \frac{3}{2}$  ( $3.87 \mu_B$  for  $g = 2$ ), and remains nearly constant down to  $10 \text{ K}$  (Figure 2). Below  $10 \text{ K}$ ,  $\mu_{\text{eff}}$  decreases to  $3.6 \mu_B$  at  $2 \text{ K}$ , which is likely

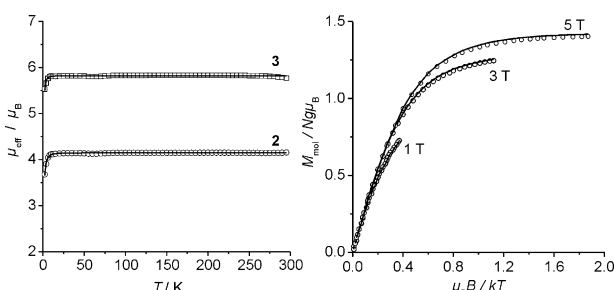


**Figure 2.** Left:  $\mu_{\text{eff}}$  versus  $T$  (left) of compounds **2** (circles) and **3** (squares); right: VTVH magnetization measurements as  $M_{\text{mol}}$  versus  $B/T$  for **2**. The solid lines represent the best fits to the experimental data.

a result of zero-field splitting. Since in all other reported two-coordinate manganese(II) compounds the magnetic moment is close to the spin-only value ( $5.92 \mu_B$ ), corresponding to their  $d^5$  high-spin configuration with  $S = \frac{5}{2}$ , the situation in **2** is rather unusual. This result led us to the initial assumption that **2** contains covalent bonds between the carbene carbon atom and the central manganese atom, leaving a radical center at both carbene moieties. On this basis, it can be understood that very strong antiferromagnetic coupling between the central  $S = \frac{5}{2}$  manganese and two  $S = \frac{1}{2}$  radical-spin carriers results in an overall  $S_T = \frac{3}{2}$  ground state. Indeed, analysis of the magnetic data leads to a good fit with  $g(\text{radical}) = 2.00$ ,  $g(\text{Mn}) = 2.10$ , and  $J = -504 \text{ K}$  (see the Supporting Information). It should be noted that because no temperature dependence of  $\mu_{\text{eff}}$  could be observed up to room temperature, the  $J$  values represent a lower limit of the coupling strength. Variable temperature/variable field (VTVH) magnetization measurements of **2** (Figure 2, right) can be well simulated with essentially the same parameters derived from the susceptibility data, thus confirming the model. The nesting of the isofield lines clearly evidences the presence of anisotropy and reveals a positive sign of the zero-field splitting parameter  $D = +2.0 \text{ K}$ .

Figure 3 shows the energy-level diagrams along with the experimentally observed and simulated EPR spectra of **2** using the parameters  $S = \frac{3}{2}$ ,  $g = 1.97$ ,  $D = 1.937 \text{ K}$  ( $13475 \text{ G}$ ), and  $E = 0.01 \text{ K}$  ( $\approx 100 \text{ G}$ ). It was necessary to add about 2% free radical ( $S = \frac{1}{2}$ ) impurity signal for an optimum fit with the observed spectrum. Once again, the simulated and the experimentally observed spectra fit quite well and are in good agreement with the magnetization data. The sign of  $D$  was confirmed by comparison of the relative line intensities in the spectra obtained at  $290$  and  $140 \text{ K}$  (see Figure S3 in the Supporting Information). The simple two-line spectrum of **2** is attributed to the energy of  $D$  being much higher than the X-band quantum, thus only two transitions can be achieved. When  $D$  is smaller than the microwave quantum, many transitions become accessible at the X-band. Further proof of the spin state of **2** was achieved using exhaustive simulations for  $S = 2$  and  $\frac{5}{2}$  models with varying values of  $D$ ,  $E$ , and  $g$ . The best-fit simulations using  $S = 2$  and  $S = \frac{5}{2}$  along with the experimental spectrum of **2** at  $140 \text{ K}$  are shown in Figure S4 in the Supporting Information. These results show unambiguously that  $S = \frac{3}{2}$  is the only model that gives an acceptable fit

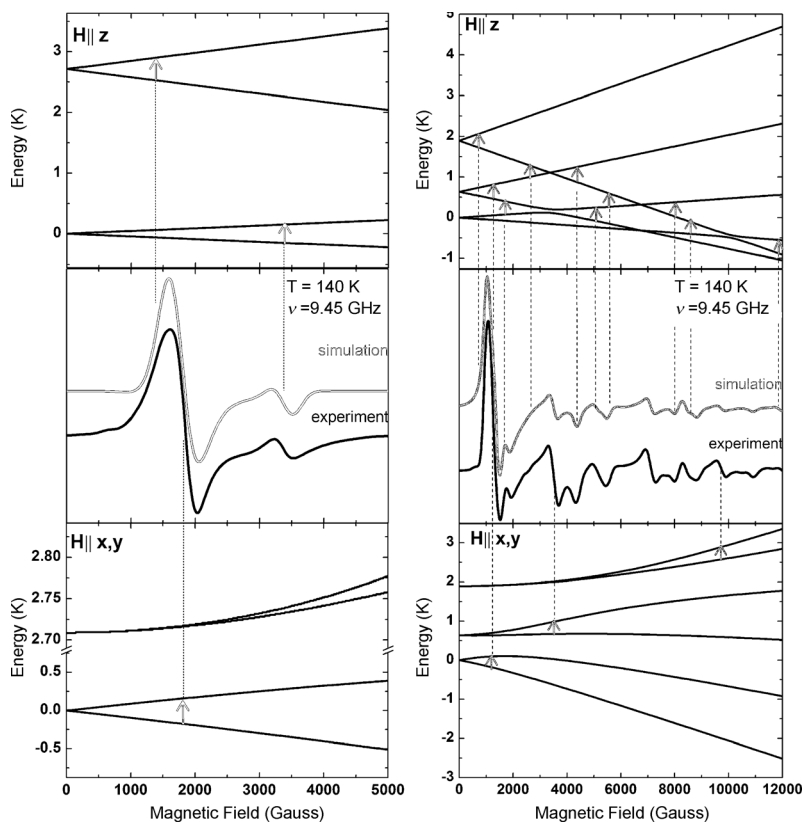


**Figure 3.** Experimentally observed and simulated spectra of **2** (left) and **3** (right) with the energy-level diagram for the principal symmetry axis,  $H \parallel z$ , and the perpendicular  $X, Y$  directions. The arrows mark the EPR transition assignments.

to the observed spectra of **2**, regardless of the values of  $D$ ,  $E$ , and  $g$ . DFT calculations with the ORCA program package<sup>[7]</sup> (B3LYP functional) on the experimental structure of **2** shows that spin–spin and spin–orbit coupling give the main contributions to  $D$  and  $E$ . The calculated values for **2** are in good agreement with the values obtained by EPR measurements (Table S7).

In order to gain further insight into the electronic fine structure of the ground state of compound **2**, we performed ab initio calculations on the experimental structure. Relativistic CASSCF/CASPT2 calculations<sup>[8]</sup> which employ an active space that consists of five  $d$  orbitals of Mn and two orbitals of the radicals, show clearly that the ground state is a spin quartet. Active orbitals are given in the Supporting Information (Table S2). The first three and the fifth active orbitals of gerade symmetry are of Mn  $3d$  type, the fourth one and the sixth are bonding and antibonding combinations

between one  $d$  orbital and two  $2p$  orbitals of the radicals ( $R_g$ ). The orbital of ungerade symmetry is a direct bonding orbital between the radicals ( $R_u$ ). The wave function of the spin ground state is truly multiconfigurational, with important contributions from several configurations (Table 1). Interestingly, the Mulliken spin population analysis shows four spins “up” on the Mn center (main configuration), while one spin of opposite projection is equally distributed among the two “carbene” carbon atoms, with small tails on the nitrogen atoms. Other important configurations arise mainly from the biradical structure. Two low-lying spin sextet states originate from the reversal of the spin of ungerade radical orbital, and to a complete coupling between the radicals, leaving the initial  $S = 5/2$  of the  $Mn^{II}$ .

Table 1 shows that the main contribution to the  $S = 3/2$  ground state is given by a *single-radical electronic configuration* with six electrons in Mn  $3d$  orbitals and one electron in the orbital delocalized between two radicals ( $R_g$  and  $R_u$ ). The magnetic structure in this configuration is described by Heisenberg exchange interaction between the radical  $S = 1/2$  in the  $R_u$  orbital and the  $S = 2$  of the  $d^6 Mn^I$  core. One should note, however, that the mixing of biradical electronic configurations is important. Therefore, the structure of magnetic states cannot be described within a conventional exchange model, but requires a full

configuration interaction calculation. To understand the large separation between the  $S = 3/2$  ground state and the excited states, clearly seen in the magnetism of **2**, we can consider only the dominant configuration 1 in Table 1. This configuration is characterized by exchange interaction  $-JS_s$  between  $s = 1/2$  of the radical spin delocalized in the orbital  $R_u$  and  $S = 2$  of the  $Mn^I$  core. In this model, the separation between the  $S = 3/2$  ground state and the excited  $S = 5/2$  is obtained as  $5/2|J|$ , where  $J$  can be of the order of hundreds or thousands of wavenumbers.

The geometry of an isolated molecule of compound **2** was optimized using different levels of theory (BP86/TZVPP and TPSS/TZVPP) for the quartet and sextet states. The calculations suggest that the quartet state is 2.4 kcal mol<sup>-1</sup> (BP86/TZVPP) and 2.3 kcal mol<sup>-1</sup> (TPSS/TZVPP) lower in energy than the sextet state, which is in agreement with the experimentally observed magnetic moment. The theoretical values for the bond lengths and bond angles of the quartet and sextet state are not very different from each other and agree reasonably well with the experimental data, except for the dihedral angle N1-C1-C1'-N1'. Figure 1 shows the calculated values at BP86/TZVPP. The data at TPSS/TZVPP, which are very similar, and the complete set of coordinates are given in the Supporting Information. The optimized structure of the quartet state has a dihedral angle N1-C1-C1'-N1' of 127.8°, which deviates significantly from  $C_i$  symmetry observed in the crystal structure. However,  $C_i$  symmetry is adopted only in the

**Table 1:** Main configurations that form the ground state of compound **2**.

	Active orbitals gerade	Active orbitals ungerade	Coefficient	Electronic configuration
1	$\uparrow\uparrow\downarrow\downarrow\downarrow$	$\downarrow$	0.783	$d^6-R_u^1$
2	$\uparrow\uparrow\downarrow\downarrow\uparrow$	$\downarrow$	-0.383	$d^5-R_g^1-R_u^1$
3	$\uparrow\uparrow\uparrow\downarrow\uparrow$	$\downarrow$	-0.095	$d^5-R_g^1-R_u^1$
4	$\uparrow\uparrow\uparrow\uparrow\downarrow$	$\downarrow$	-0.322	$d^5-R_g^1-R_u^1$
5	$\uparrow\uparrow\downarrow\downarrow\uparrow$	$\downarrow$	0.353	$d^4-R_g^2-R_u^1$

sextet state when an isolated molecule is optimized. The calculation of the quartet state with enforced  $C_i$  symmetry gave an energy that is only 2.5 kcal mol<sup>-1</sup> higher than that of the equilibrium form. As we know that compound **2** has a quartet ground state in solid phase, as evidenced from the SQUID magnetic measurement and EPR spectroscopy, it is conceivable that intermolecular interactions enforce  $C_i$  symmetry. Figure 4 shows the spin density and the three singly occupied orbitals of the quartet state of **2**, which are mainly valence  $d$  orbitals at the manganese atom.

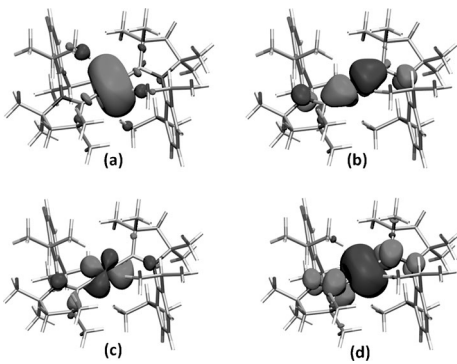


**Figure 4.** a–c) Shape of the three energetically highest lying singly occupied orbitals of the quartet state of **2** with (excess)  $\alpha$  electrons. d) Calculated spin density of the quartet state of **2**.

Reactivity studies of two-coordinate manganese compounds are still in their infant stage. However, compound **2** acts as an effective dihydrogen splitter at room temperature. The passing of dihydrogen gas at room temperature through a solution of **2** in toluene affords  $(\text{cAACl})_2\text{Mn}$  (**3**) as an alizarin-crimson-colored product in a few seconds (see Figure S12 in the Supporting Information). The hydrogen molecule was split homolytically by the two radical centers connected by Mn to produce **3**. Such an activation of the enthalpically strong H–H bond is of high interest for chemists and has been widely studied for a variety of systems. But in most of the studies, dihydrogen activation took place at the transition-metal centers. However, this chemistry has been extended to nonmetallic systems too. Power and co-workers showed that digermyne and distannyne compounds cleave molecular hydrogen at room temperature.<sup>[9]</sup> Moreover, under the irradiation of UV light, fullerenes and fullerene anions split dihydrogen at room temperature.<sup>[10]</sup> Most notably, in recent years dihydrogen cleavage has been extensively studied at frustrated Lewis pairs (FLPs) after Stephan and co-workers reported the reversible heterolytic dihydrogen splitting using intramolecular phosphine-borane pairs.<sup>[11]</sup> Apart from these investigations, dihydrogen cleavage at a single carbon center remained elusive until Bertrand and co-workers reported the oxidative addition of a hydrogen molecule at cyclic and acyclic alkyl(amino)carbene centers. Bertrand attributed this ability to a resemblance between singlet carbene and a transition-metal center.<sup>[12]</sup> Even though NHCs on their own lack this interesting ability, as a Lewis base component of FLPs they take part in the cleavage of dihydrogen.<sup>[13]</sup> In the light of these ongoing efforts, our

present result, which shows the splitting of dihydrogen at room temperature by Mn-bridged delocalized carbon radical centers, opens a new direction in this active field of chemistry. Dihydrogen cleavage by a cyclic alkyl(amino)carbene occurs upon the passing of dihydrogen gas through the solution of the carbene for 5 h at 35 °C.<sup>[12]</sup> Herein, we report that such a cyclic alkyl(amino)carbene, when bound to the Mn center as a delocalized radical ligand, can split dihydrogen within a few seconds at 25 °C. Experimental as well as theoretical studies of the mechanism of hydrogen cleavage by **2** are under way. The calculations suggest that the reaction **2** + H<sub>2</sub> → **3** is weakly exergonic by  $\Delta G^{298} = -6.2$  kcal mol<sup>-1</sup> at room temperature.

The molecular structure of **3** is shown in Figure 5. The C–Mn–C bond angle is 180°. The geometry around the carbene carbon atom is tetrahedral, thus unambiguously showing the

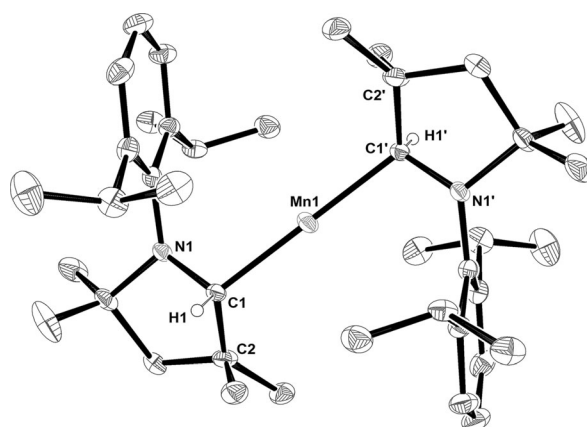


**Figure 5.** Molecular structure of compound **3**. Hydrogen atoms and solvent molecule (toluene) are omitted for clarity. Anisotropic displacement parameters are depicted at the 50% probability level. Selected experimental [calculated at BP86/def2-TZVPP] bond lengths [Å] and angles [°]: Mn1–C1 2.106(2) [2.102; 2.104], C1–C2 1.534(2) [1.548; 1.550], C1–N1 1.478(2) [1.466; 1.478], C1–Mn1–C1' 180 [163.2], C2–C1–N1 99.43(14) [102.6; 102.9], C2–C1–Mn1 121.48(14) [118.0; 121.2], N1–C1–Mn1 104.66(12) [106.5; 119.9].

presence of the hydrogen atoms. The C–Mn bond length is 2.106(2) Å, which is significantly longer than the corresponding value in the precursor **2** (1.9655(14) Å). Compound **3** is stable for several days at room temperature under an inert atmosphere but decomposes within a few seconds on exposure to air. Moreover, the product of the reaction between **2** and molecular hydrogen renders **3** in a sextet spin ground state (observed  $\mu_{\text{eff}} = 5.82 \mu_B$ , Figure 2), reflecting an unusual transition from overall  $S_T = ^3/2$  of **2** to  $S = ^5/2$  of **3** as a result of the quenching of the radical nature of the carbene ligand. Figure 5 gives the calculated bond lengths and angles at BP86/def2-TZVPP for the sextet state of **3**. The calculations give a bending angle C1–Mn1–C1' of 163.2°, while the X-ray analysis shows a linear geometry at manganese. This difference might be caused by solid-state effects, the calculated energy that is required to achieve a linear geometry of **3** is only 1.1 kcal mol<sup>-1</sup>.

The EPR spectrum of **3** at 140 K is shown in Figure 3. The simulated spectrum was obtained using  $S = ^5/2$ ,  $g = 2.00$ ,  $D =$

0.45 K (3130 G), and  $E = 0.015$  K (105 G). The hyperfine ( $A$ ) term was omitted in the simulations, because no hyperfine structure was observed, likely because of fast electron exchange. The spectra of **3** are rather complex and show a total of 13 lines, some of which are slightly distorted, but the agreement between the experimentally observed and simulated spectra is quite satisfactory. A slight discrepancy in the intensity of the transition around  $g = 2.00$  (3350 gauss) is due to a very minute (< 1%)  $S = \frac{1}{2}$  free-radical impurity. The sign of  $D$  was confirmed again by comparison of the relative line intensities in the spectra at 290 and 140 K (see Figure S5 in the Supporting Information). DFT calculations with B3LYP functional show that the contribution of the spin–spin coupling to  $D$  and  $E$  is one order of magnitude larger than that of the spin–orbit coupling (see Tables S3 and S7 in the Supporting Information).

In conclusion, an intensely purple-colored linear (cAAC)<sub>2</sub>Mn complex (**2**), which features a two-coordinate manganese atom, was synthesized in high yield. The main contribution to the  $S = \frac{3}{2}$  ground state of **2** originates from the antiferromagnetic coupling between  $S = 2$  Mn<sup>I</sup> and one  $S = \frac{1}{2}$  radical spin that is delocalized on two “carbene” carbon atoms. Another important contribution to the quartet state comes from the antiferromagnetic coupling between the central  $S = \frac{5}{2}$  Mn<sup>II</sup> and the two  $S = \frac{1}{2}$  radical spins. The calculations suggest that the quartet state has the lowest energy, which is in good agreement with the experimental value of the magnetic moment. Complex **2** shows excellent reactivity in splitting dihydrogen at room temperature to give (cAAACH)<sub>2</sub>Mn (**3**), which has the spin ground state  $S = \frac{5}{2}$ .

Received: May 29, 2013

Revised: July 17, 2013

Published online: September 13, 2013

**Keywords:** coordination modes · cyclic alkyl(amino)carbene · density functional calculations · dihydrogen splitting · manganese

- [1] a) J. Chai, H. Zhu, A. C. Stückl, H. W. Roesky, J. Magull, A. Bencini, A. Caneschi, D. Gatteschi, *J. Am. Chem. Soc.* **2005**, *127*, 9201–9206; b) L. Sorace, Ch. Golze, D. Gatteschi, A. Bencini, H. W. Roesky, J. Chai, A. C. Stückl, *Inorg. Chem.* **2006**, *45*, 395–400.

- [2] a) K. C. Mondal, H. W. Roesky, M. C. Schwarzer, G. Frenking, B. Niepötter, H. Wolf, R. Herbst-Irmer, D. Stalke, *Angew. Chem.* **2013**, *125*, 3036–3040; *Angew. Chem. Int. Ed.* **2013**, *52*, 2963–2967; b) K. C. Mondal, H. W. Roesky, M. C. Schwarzer, G. Frenking, I. Tkach, H. Wolf, D. Kratzert, R. Herbst-Irmer, B. Niepötter, D. Stalke, *Angew. Chem.* **2013**, *125*, 1845–1850; *Angew. Chem. Int. Ed.* **2013**, *52*, 1801–1805; c) M. Melaimi, M. Soleilhavoup, G. Bertrand, *Angew. Chem.* **2010**, *122*, 8992–9032; *Angew. Chem. Int. Ed.* **2010**, *49*, 8810–8849; d) C. D. Martin, M. Soleilhavoup, G. Bertrand, *Chem. Sci.* **2013**, *4*, 3020–3030; e) V. Lavallo, Y. Canac, C. Präsang, B. Donnadieu, G. Bertrand, *Angew. Chem.* **2005**, *117*, 5851–5855; *Angew. Chem. Int. Ed.* **2005**, *44*, 5705–5709; f) R. Jazzar, R. D. Dewhurst, J.-B. Bourg, B. Donnadieu, Y. Canac, G. Bertrand, *Angew. Chem.* **2007**, *119*, 2957–2960; *Angew. Chem. Int. Ed.* **2007**, *46*, 2899–2902.
- [3] P. P. Power, *Chem. Rev.* **2012**, *112*, 3482–3507.
- [4] a) W. M. Reiff, A. M. LaPointe, E. H. Witten, *J. Am. Chem. Soc.* **2004**, *126*, 10206–10207; b) J. M. Zadrozny, D. J. Xiao, M. Atanasov, G. J. Long, F. Grandjean, F. Neese, J. R. Long, *Nat. Chem.* **2013**, *5*, 577–581.
- [5] a) N. H. Buttrus, C. Eaborn, P. B. Hitchcock, A. C. Sullivan, *J. Chem. Soc. Chem. Commun.* **1985**, 1380–1381; b) A. Alberola, V. L. Blair, L. M. Carrella, W. Clegg, A. R. Kennedy, J. Klett, R. E. Mulvey, S. Newton, E. Rentschler, L. Russo, *Organometallics* **2009**, *28*, 2112–2118; c) R. A. Andersen, E. Carmona-Guzman, J. F. Gibson, G. Wilkinson, *J. Chem. Soc. Dalton Trans.* **1976**, 2204–2211. For more references, see Ref. [17] in the Supporting Information.
- [6] The calculated quartet state of the isolated molecule of **2** has  $C_1$  symmetry, in which the bond lengths and angles of the two ligands are slightly different from each other.
- [7] a) F. Neese, *J. Chem. Phys.* **2007**, *127*, 164112; b) F. Neese, *J. Am. Chem. Soc.* **2006**, *128*, 10213–10222.
- [8] F. Aquilante, L. De Vico, N. Ferré, G. Ghigo, P. Å. Malmqvist, P. Neogrady, T. B. Pedersen, M. Pitoňák, M. Reiher, B. O. Roos, L. Serrano-Andres, M. Urban, V. Veryazov, R. Lindh, *J. Comput. Chem.* **2010**, *31*, 224–247.
- [9] a) G. H. Spikes, J. C. Fettinger, P. P. Power, *J. Am. Chem. Soc.* **2005**, *127*, 12232–12233; b) Y. Peng, M. Brynda, B. D. Ellis, J. C. Fettinger, E. Rivard, P. P. Power, *Chem. Commun.* **2008**, 6042–6044.
- [10] B. J. Li, Z. Xu, *J. Am. Chem. Soc.* **2009**, *131*, 16380–16382.
- [11] G. C. Welch, R. R. San Juan, J. D. Masuda, D. W. Stephan, *Science* **2006**, *314*, 1124–1126.
- [12] a) G. D. Frey, V. Lavallo, B. Donnadieu, W. W. Schoeller, G. Bertrand, *Science* **2007**, *316*, 439–441; b) D. Martin, M. Soleilhavoup, G. Bertrand, *Chem. Sci.* **2011**, *2*, 389–399.
- [13] P. A. Chase, D. W. Stephan, *Angew. Chem.* **2008**, *120*, 7543–7547; *Angew. Chem. Int. Ed.* **2008**, *47*, 7433–7437.